

# **Bayesian Retinex Underwater Image Enhancement**

*An MSc. Project Report Submitted  
in Partial Fulfillment of the Requirements  
for the Degree of*

**Master of Science in Mathematics & Computing**

*by*

**Rahim Khan**  
(222123040)

*under the guidance of*

**Dr. Rajen Kumar Sinha**



*to the*

**DEPARTMENT OF MATHEMATICS**

**INDIAN INSTITUTE OF TECHNOLOGY GUWAHATI  
GUWAHATI - 781039, ASSAM**

# CERTIFICATE

*This is to certify that the work contained in this thesis entitled “**Bayesian Retinex Underwater Image Enhancement**” is a bonafide work of **Rahim Khan (Roll No. 222123040)**, carried out in the Department of Mathematics, Indian Institute of Technology Guwahati under my supervision and that it has not been submitted elsewhere for a degree.*

Supervisor: **Dr. Rajen Kumar Sinha**

Assistant/Associate Professor,

May, 2024

Department of Mathematics,

Guwahati.

Indian Institute of Technology Guwahati, Assam.

# Abstract

*The paper proposes a new Bayesian retinex algorithm for enhancing single underwater images. A simple color correction approach is first applied to remove color casts and recover natural colors. A maximum a posteriori formulation imposes multi-order gradient priors on the reflectance and illumination components of the color-corrected image. The  $l_1$  norm models piecewise/piecewise linear priors on the reflectance, while the  $l_2$  norm enforces spatial smoothness priors on the illumination. This formulation breaks down the enhancement problem into two denoising subproblems that can be efficiently optimized. The method operates pixelwise without requiring prior knowledge of underwater conditions. Experimental results show the proposed approach outperforms traditional and leading methods for color correction, naturalness preservation, detail enhancement, and artifact/noise suppression on qualitative and quantitative assessments. The method shows promising applications for challenging underwater image enhancement scenarios. In summary, it introduces a novel Bayesian retinex model with effective priors and a decomposition approach for high-quality single underwater image enhancement.*

# Contents

<b>List of Figures</b>	<b>iv</b>
<b>List of Tables</b>	<b>vi</b>
<b>1 Introduction</b>	<b>1</b>
<b>2 RGB and HSV Color spaces</b>	<b>3</b>
2.1 RGB Color Space[Bur09] . . . . .	3
2.2 HSV Color Space . . . . .	5
<b>3 Color Correction</b>	<b>1</b>
<b>4 ADMM Algorithm</b>	<b>3</b>
4.1 Convex Functions . . . . .	3
4.2 ADMM Algorithm . . . . .	4
<b>5 Metrics</b>	<b>6</b>
5.1 Underwater Image Quality Metric (UIQM) . . . . .	6
5.1.1 UICM . . . . .	6
5.1.2 UISM . . . . .	8
5.1.3 UIConM . . . . .	8
5.2 Underwater Color Image Quality Evaluation Metric(UCIQE) . . . . .	9
5.3 Colorfulness,Contrast and Fog-density (CCF) . . . . .	10

5.3.1	Colorfulness Index . . . . .	10
5.3.2	Contrast Index . . . . .	11
5.3.3	Fog Density Index . . . . .	12
5.4	Entropy . . . . .	13
<b>6</b>	<b>Bayesian Retinex Underwater Image Enhancement</b>	<b>15</b>
6.1	Model Construction . . . . .	15
6.1.1	Step 1 : Color Correction :- . . . . .	15
6.1.2	Step 2 : RGB to HSV conversion :- . . . . .	16
6.1.3	Step 3 : Model Description :- . . . . .	16
6.1.4	Step 4 : Objective Function :- . . . . .	19
6.1.5	Step 5 : Numerical Optimization :- . . . . .	20
6.1.6	Step 6 : Update for P-1 :- . . . . .	21
6.1.7	Step 7 : Update for P-2 :- . . . . .	21
6.1.8	Step 9 : Update for P-3 :- . . . . .	21
6.1.9	Algorithm :- . . . . .	22
6.1.10	Gamma Correction :- . . . . .	22
6.1.11	Image Reconstruction :- . . . . .	22
6.1.12	Conversion from HSV to RGB :- . . . . .	23
6.2	Results . . . . .	23
6.2.1	Comparison with other algorithms . . . . .	23
6.2.2	List algorithms for comparison . . . . .	25
<b>7</b>	<b>Conclusion and Future Work</b>	<b>34</b>
7.1	Conclusion . . . . .	34
7.2	Future Work . . . . .	35
<b>References</b>		<b>37</b>

# List of Figures

1.1 Underwater Image formation . . . . .	2
2.1 Representation of the RGB color space as a three-dimensional unit cube. The primary colors red (R), green (G), and blue (B) form the coordinate system. The “pure” red color (R), green (G), blue (B), cyan (C), magenta (M), and yellow (Y) lie on the vertices of the color cube. All the shades of gray, of which K is an example, lie on the diagonal between black S and white W. . . . .	4
2.2 HSV Color Space . . . . .	5
2.3 HSV Color Space . . . . .	6
4.1 Convex Function . . . . .	3
6.1 right unprocessed and left processed . . . . .	24
6.2 right unprocessed and left processed . . . . .	25
6.3 raw and processed image . . . . .	26
6.4 Clahe [vas13] and Grey World [Buc80] . . . . .	26
6.5 SSR [Job15a] and MSR [Job15b] . . . . .	28
6.6 MSRPCP [San12] and MAXRGB [Lan77] . . . . .	28
6.7 WCID [CC12] and white balance [M07] . . . . .	28
6.8 (A) & (B) . . . . .	29
6.9 (C) & (D) . . . . .	29
6.10 for image A . . . . .	30

6.11 for image B . . . . .	31
6.12 for image C . . . . .	32
6.13 for image D . . . . .	33

# List of Tables

6.1 Comparison of Image Processing Methods . . . . .	26
6.2 Recovered Edges by different algorithms . . . . .	27



# Chapter 1

## Introduction

Underwater imaging is a crucial research field, given the abundant resources present in oceans, rivers, and lakes. However, underwater image processing poses unique challenges due to the complex physical properties of the underwater environment. Factors such as color distortion and contrast degradation arise from light absorption and scattering in water.

The underwater optical imaging model is explained, illustrating that captured light consists of three main components: direct, forward scattering, and backward scattering. The forward scattering component causes blurred structures in underwater images, while the backward scattering component obscures image edges and details. Additionally, color distortion results from the varying absorption rates of different wavelengths of light in water.

To address these challenges, the paper proposes a solution – a Bayesian retinex algorithm with multiorder gradient priors for both reflectance and illumination. This algorithm aims to enhance single underwater images by mitigating color distortion and contrast degradation, ultimately striving to produce high-quality underwater images for further processing.

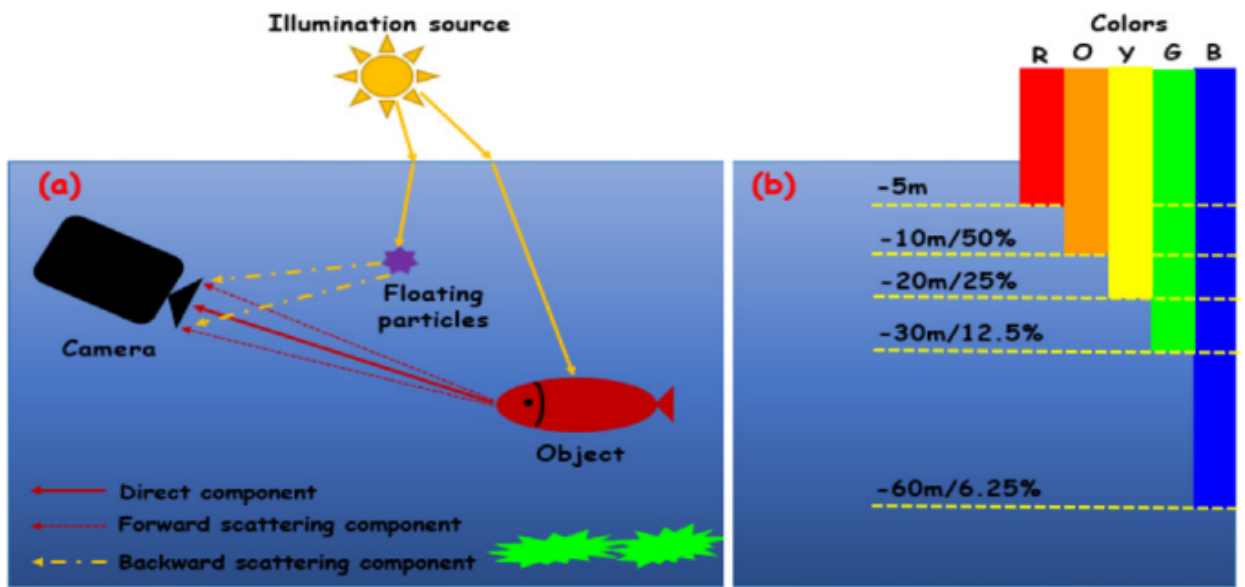


**Fig. 1.1:** Underwater Image formation

# Chapter 2

## RGB and HSV Color spaces

### 2.1 RGB Color Space[Bur09]

The RGB color schema encodes colors as combinations of the three primary colors: red (R), green (G), and blue (B). This scheme is widely used for transmission, representation, and storage of color images on both analog devices such as television sets and digital devices such as computers, digital cameras, and scanners. For this reason, many image-processing and graphics programs use the RGB schema as their internal representation for color images, and most RGB is an additive color system, which means that all colors start with black and are created by adding the primary colors. You can think of color formation in this system as occurring in a dark room where you can overlay three beams of light—one red, one green, and one blue—on a sheet of white paper. To create different colors, you would modify the intensity of each of these beams independently. The distinct intensity of each primary color beam controls the shade and brightness of the resulting color. The colors gray and white are created by mixing the three primary color beams at the same intensity. The RGB color space can be visualized as a three-dimensional unit cube in which the three primary colors form the coordinate axis. The RGB values are positive and lie in the range  $[0, C_{max}]$ ; for most digital images,  $C_{max} = 255$ . Every possible color  $C_i$  corresponds to a point

within the RGB color cube of the form

$$C_i = (R_i, G_i, B_i)$$

where  $R_i, G_i, B_i \leq C_{max}$ . RGB values are often normalized to the interval  $[0, 1]$  so that the resulting color space forms a unit cube as shown in the figure. The point  $S = (0, 0, 0)$  corresponds to the color black,  $W = (1, 1, 1)$  corresponds to the color white, and all the points lying on the diagonal between  $S$  and  $W$  are shades of gray created from equal color components  $R = G = B$ .

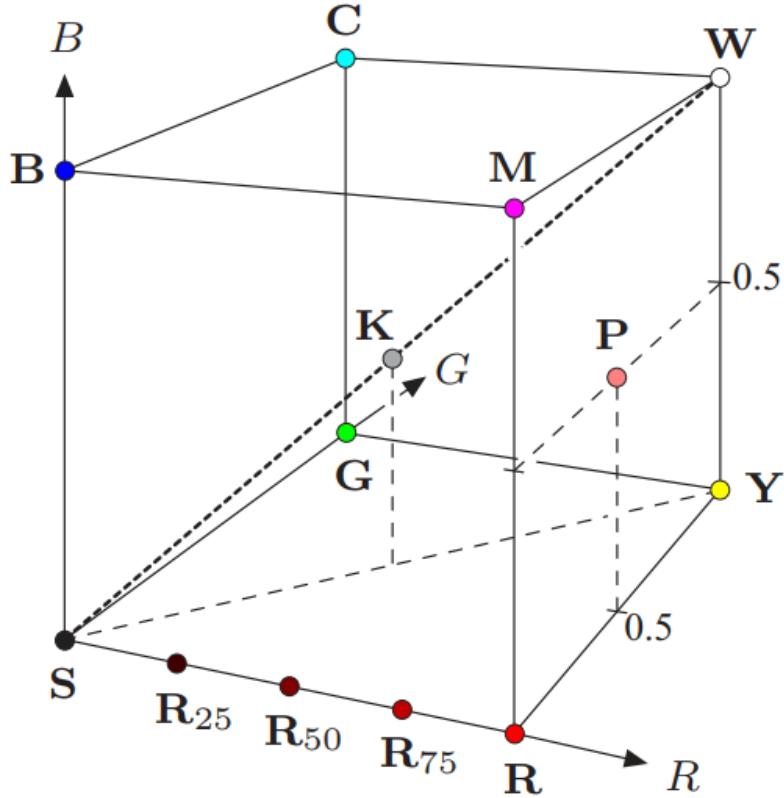


**Fig. 2.1:** Representation of the RGB color space as a three-dimensional unit cube. The primary colors red (R), green (G), and blue (B) form the coordinate system. The “pure” red color (R), green (G), blue (B), cyan (C), magenta (M), and yellow (Y) lie on the vertices of the color cube. All the shades of gray, of which K is an example, lie on the diagonal between black S and white W.

## 2.2 HSV Color Space

In the HSV color space, colors are specified by the components *hue*, *saturation*, and *value*.

The HSV color space is traditionally shown as an upside-down, six-sided pyramid, where the vertical axis represents the V (brightness) value, the horizontal distance from the axis the S (saturation) value, and the angle the H (hue) value. The black point is at the tip of the pyramid and the white point lies in the center of the base. The three primary colors red, green, and blue and the pairwise mixed colors yellow, cyan and magenta are the corner points of the base. While this space is often represented as a pyramid, according to its mathematical definition, the space is actually a cylinder. In HSV color space H represents the angle from Red color point in anticlockwise

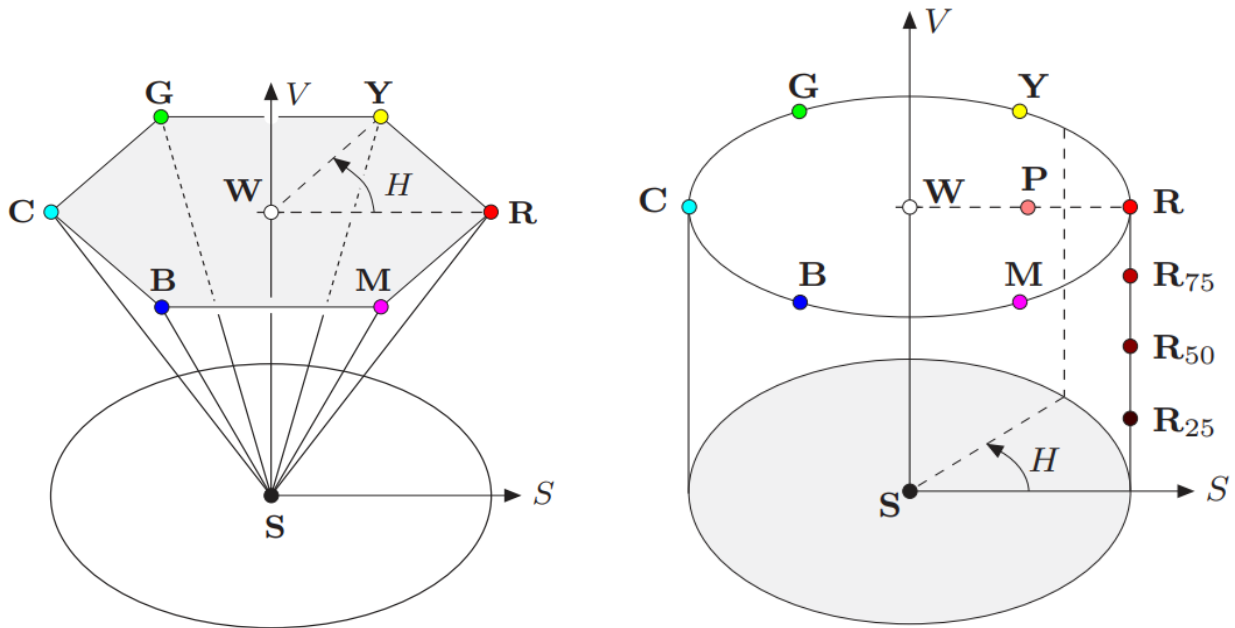


**Fig. 2.2:** HSV Color Space

direction, S represents the distance of the point from the central axis and V is the distance of the point from the bottom.

The conversion process is defined as follows →

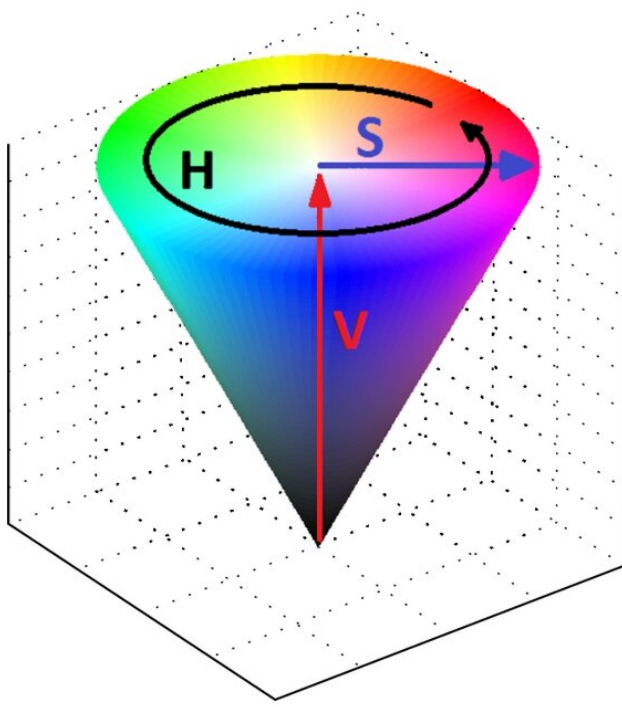


**Fig. 2.3:** HSV Color Space

for any given color pixel having RGB values  $P(R,G,B)$

define  $C_{high} = \max(R, G, B)$  ,  $C_{low} = \min(R, G, B)$  and  $C_{rng} = C_{high} - C_{low}$

$$S_{HSV} = \begin{cases} \frac{C_{rng}}{C_{high}} & \text{for } C_{high} > 0 \\ 0 & \text{otherwise} \end{cases}$$

$$V_{HSV} = \frac{C_{high}}{C_{max}}$$

$$R' = \frac{C_{high} - R}{C_{rng}}, B' = \frac{C_{high} - B}{C_{rng}}, G' = \frac{C_{high} - G}{C_{rng}}$$

$$H' = \begin{cases} B' - G' & \text{if } R = C_{high} \\ R' - B' & \text{if } G = C_{high} \\ G' - R' & \text{if } B = C_{high} \end{cases}$$

$$H_{HSV} = 60^\circ \times \begin{cases} H' + 6 & \text{if } H' < 0 \\ H' & \text{otherwise} \end{cases}$$

# Chapter 3

## Color Correction

The green light travels the longest distance through water for its shortest wavelength, most underwater images appear green or blue . To address the color cast, a color correction based on statistical method is adopted we define s as observed underwater image. The operation process is as follows. First, the mean value and the mean squared error are computed in RGB(Red,Green,Blue) channels of s respectively.

second the maximum and minimum of each channel is calculated by →

$$S_{max}^c = S_{mean}^c + \mu S_{var}^c$$

$$S_{min}^c = S_{mean}^c - \mu S_{var}^c$$

where  $c \in \{R,G,B\}$ ,  $S_{mean}^c$  and  $S_{var}^c$  are mean value and mean square error of the channel c respectively.  $\mu$  is the parameter to control the image dynamic;  $S_{max}^c$  and  $S_{min}^c$  are the maximum and minimum of the c channel. Finally, the color corrected image is obtained by

$$S_{CR}^c = \frac{S^c - S_{min}^c}{S_{max}^c - S_{min}^c} \times 255$$

where  $S_{CR}^c$  is the color corrected image. On further simplification  $\rightarrow$

$$\begin{aligned}
S_{CR}^c &= \frac{S^c - S_{min}^c}{S_{max}^c - S_{min}^c} \times 255 \\
&= \frac{S^c - S_{mean}^c + \mu S_{var}^c}{S_{mean}^c + \mu S_{var}^c - S_{mean}^c + \mu S_{var}^c} \times 255 \\
&= \frac{S^c - S_{mean}^c + \mu S_{var}^c}{2\mu S_{var}^c} \times 255 \\
&= \frac{255}{2} \times \left( 1 + \frac{S^c - S_{mean}^c}{\mu S_{var}^c} \right).
\end{aligned}$$

$$S_{CR}^c = \frac{255}{2} \times \left( 1 + \frac{S^c - S_{mean}^c}{\mu S_{var}^c} \right)$$

now this formula can be used for color correction of the underwater images.

\* I have used standard deviation instead of variance in the color correction for better results.

Ref-[Din14]

# Chapter 4

## ADMM Algorithm

### 4.1 Convex Functions

**Definition :** – A function  $\mathcal{F} : \mathbb{R}^n \rightarrow \mathbb{R}$  is convex if its domain is convex set and for all  $x, y \in \mathbb{R}^n$  and  $\forall \lambda \in [0, 1]$ , we have

$$\mathcal{F}(\lambda x + (1 - \lambda)y) \leq \lambda\mathcal{F}(x) + (1 - \lambda)\mathcal{F}(y) \quad (1)$$

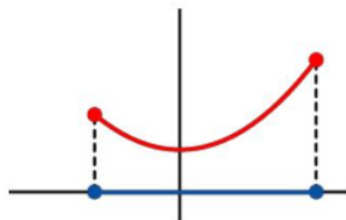


**Fig. 4.1:** Convex Function

$$\mathcal{F}(\lambda x + (1 - \lambda)y) < \lambda\mathcal{F}(x) + (1 - \lambda)\mathcal{F}(y) \quad (2)$$

if it satisfies the above inequality (2) for its domain then it is called the strictly convex function.

**Theorem:-** Consider an unconstrained optimization problem

$$\min \mathcal{F}(x)$$

$$s.t \ x \in \mathbb{R}^n,$$

where  $\mathcal{F}$  is convex and differentiable . Then any point  $\bar{x}$  that satisfies  $\nabla\mathcal{F}(\bar{x}) = 0$  is global minimum.

## 4.2 ADMM Algorithm

ADMM stands for Alternating Direction Method of Multipliers. It is an optimization algorithm used for solving convex optimization problems. ADMM aims to minimize an objective function subject to some constraints by decomposing the problem into smaller subproblems that can be solved iteratively. The algorithm alternates between updating the primal variables, the dual variables, and a Lagrange multiplier.

Consider the following optimization problem

$$\min_x \mathcal{F}(x) + \mathcal{G}(z)$$

$$\text{subject to } \mathcal{A}x + \mathcal{B}z = c$$

where  $x \in \mathbb{R}^n$ ,  $z \in \mathbb{R}^m$ ,  $\mathcal{A} \in \mathbb{R}^{p \times n}$ ,  $\mathcal{B} \in \mathbb{R}^{p \times m}$  and  $c \in \mathbb{R}^p$ . Here we are assuming that  $\mathcal{F}$  and  $\mathcal{G}$  are convex and differentiable functions. Now define the augmented langrangian

$$\mathcal{L}_\rho(x, z, y) = \mathcal{F}(x) + \mathcal{G}(z) + y^T(\mathcal{A}x + \mathcal{B}z - c) + \frac{\rho}{2}\|\mathcal{A}x + \mathcal{B}z - c\|_2^2$$

ADMM consists of the iterations

$$\begin{aligned} x^{k+1} &= \arg \min_x \mathcal{L}_\rho(x, z^k, y^k) \\ z^{k+1} &= \arg \min_z \mathcal{L}_\rho(x^{k+1}, z, y^k) \\ y^{k+1} &= y^k + \rho(\mathcal{A}x^{k+1} + \mathcal{B}z^{k+1} - c) \end{aligned}$$

where  $\rho > 0$

Ref- [PE10]

# Chapter 5

## Metrics

### 5.1 Underwater Image Quality Metric (UIQM)

Underwater Image Quality Measure. The UIQM is a linear composition of three underwater image attribute measures: Underwater Image Sharpness Measure (UISM), Underwater Image Contrast Measure (UIConM), and Underwater Image Colorfulness Measure (UICM). The UIQM measures three important underwater image quality criterions: colorfulness, sharpness, and contrast, and the three weighted parameters are empirically recommended to be 0.2953, 3.5753, and 0.0282, respectively. The higher UIQM values indicate a better balance among colorfulness, sharpness and contrast in the image.

#### 5.1.1 UICM

Underwater images commonly suffer from color-casting issues, where colors are distorted due to the absorption of light by water. As depth increases, colors attenuate in a predictable sequence, with red disappearing first due to its shorter wavelength. This leads to underwater images often appearing bluish or greenish. Additionally, poor lighting conditions exacerbate color desaturation. Effective enhancement algorithms for underwater images should prioritize accurate color rendition. Research indicates that natural scene colorfulness can be effectively represented using statistical values of images. Users have the flexibility to select color spaces, order statistical values, fusion

functions, and weighting coefficients for enhancement. Given that the human visual system perceives colors in opponent color planes, techniques such as using the RG and YB opponent color components are employed in underwater image enhancement algorithms, known as the Underwater Image Color Model (UICM).

$$RG = R - G$$

$$YB = \frac{R + G}{2} - B$$

where R,G,B has there usual meaning.Underwater images usually suffer from heavy noise. Therefore, instead of using the regular statistical values, the asymmetric alpha-trimmed statistical values are used for measuring underwater image colorfulness

For an image of size  $M \times N$  let  $K=M \times N$  and all the pixels in the image are sorted in increasing order. Let  $T_{\alpha_L} = \lceil \alpha_L K \rceil$  and  $T_{\alpha_R} = \lfloor \alpha_R K \rfloor$  be the number of the smallest and greatest pixel values to be trimmed or discarded from the sorted sequence The asymmetric alpha-trimmed mean is defined by

$$\mu_{\alpha,RG} = \frac{1}{K - T_{\alpha_L} - T_{\alpha_R}} \sum_{i=T_{\alpha_L}+1}^{K-T_{\alpha_R}} Intensity_{RG,i}$$

$$\sigma_{\alpha,RG}^2 = \frac{1}{N} \sum_{p=1}^N (Intensity_{RG,p} - \mu_{\alpha,RG})^2$$

Now similarly define  $\mu_{\alpha,YB}, \sigma_{\alpha,YB}^2$ . Then underwater image colorfulness measure (UICM) is calculated by the given formula →

$$UICM = -0.0268 \sqrt{\mu_{\alpha,RG}^2 + \mu_{\alpha,YB}^2} + 0.1586 \sqrt{\sigma_{\alpha,RG}^2 + \sigma_{\alpha,YB}^2}$$

### 5.1.2 UISM

In underwater photography, maintaining sharpness is challenging due to significant blurring caused by forward scattering. This degradation affects the preservation of fine details and edges in underwater images. To measure sharpness, the Sobel edge detector is employed on each RGB color component, generating an edge map. This map is then multiplied with the original image to produce a grayscale edge map, preserving only the pixels corresponding to edges. The Enhancement Measure Estimation (EME) method, suitable for images with uniform backgrounds and non-periodic patterns, is utilized to assess edge sharpness in underwater images. The UISM is formulated as

$$EME = \frac{2}{k_1 k_2} \sum_{l=1}^{k_1} \sum_{k=1}^{k_2} \log \left( \frac{I_{max,k,l}}{I_{min,k,l}} \right)$$

$$UISM = \sum_{c=1}^3 \lambda_c EME(\text{grayscale edge}_c)$$

where  $\lambda_R = 0.299$ ,  $\lambda_G = 0.587$ ,  $\lambda_B = 0.114$

### 5.1.3 UIConM

Contrast has been shown to correspond to underwater visual performance such as stereoscopic acuity . For underwater images, contrast degradation is usually caused by backward scattering . In this paper, the contrast is measured by applying the logAMEE measure on the intensity image as

$$\logAMEE = \frac{1}{k_1 k_2} \otimes \sum_{l=1}^{k_1} \sum_{k=1}^{k_2} \frac{I_{max,k,l} \ominus I_{min,k,l}}{I_{max,k,l} \oplus I_{min,k,l}} \times \log \left( \frac{I_{max,k,l} \ominus I_{min,k,l}}{I_{max,k,l} \oplus I_{min,k,l}} \right)$$

$$UIconM = \logAMEE(\text{Intensity})$$

where an image is divided into blocks  $k_1$ ,  $k_2$  and  $\ominus, \oplus, \otimes$  are the PLIP operations, introduces the entropy-like operation to the traditional Agaian measure of enhancement by engropy (AMEE), which is formulated as the average Michaelson contrast in image local regions. The PLIP operations, which provides the nonlinear representations that are consistent with human visual perceptions, are also used in the logAMEE formulation. Practically, lighting conditions are usually poor under the water. In such cases, the logAMEE is preferred for the reason that the log and PLIP operations put more emphasis on areas with low luminance.

It has been demonstrated that underwater images can be modeled as linear superposition of absorbed and scattered components. Besides, it is known that the absorption and scattering effects cause color, sharpness, and contrast degradation. Therefore, it is reasonable to use the linear superposition model for generating the overall underwater image quality measure as well. The overall underwater image quality measure is then given by

$$UIQM = 0.0282 \times UICM + 0.2953 \times UISM + 3.5753 \times UIConM$$

Ref-[Aga16]

## 5.2 Underwater Color Image Quality Evaluation Metric(UCIQE)

Underwater color images, particularly those used in pipeline monitoring or engineering surveys. These images often suffer from issues like blurriness, low contrast, and strong color casts. Selecting an appropriate metric for evaluating image quality involves considering aspects such as correlation with subjective test data, computational cost, and limitations of the experimental setup.

One consideration is whether to emphasize the blue-yellow axis in the CIELab color space, as suggested by Hasler and Suesstrunk. However, since CIELab is designed to be a uniform color space, this emphasis may not be reasonable. Additionally, it's suggested to avoid using the deviation of saturation ( $\sigma_s$ ) as a metric because it can overly highlight dark areas, which are common in underwater images due to limited lighting. The underwater color image quality

evaluation metric, UCIQE, operates in the CIELab color space. The pixel values of an image in this space are represented as  $I_p = [l_p, a_p, b_p]$ , where  $p$  ranges from 1 to  $N$ , with  $N$  being the total number of pixels in the image. Chroma (CI) is also a factor in this metric.

$$UCIQE = c_1 \times \sigma_c + c_2 \times con_l + c_3 \times \mu_s$$

for calculating UCIQE first we have to convert the image into CIELab color space.

let  $I_{M \times N}$  is the image represented in CIELab color space consists of L,a,b channels.

$$\begin{aligned} chroma_{ij} &= \sqrt{a_{ij}^2 + b_{ij}^2} \\ \mu_c &= \frac{1}{M \times N} \sum_{i=0}^{M-1} \sum_{j=0}^{N-1} chroma_{ij} \\ \sigma_c &= \sqrt{\frac{1}{M \times N} \sum_{i=0}^{M-1} \sum_{j=0}^{N-1} (chroma_{ij}^2 - \mu_c^2)} \\ saturation_{ij} &= \frac{chroma_{ij}}{l_{ij}} \\ \mu_s &= \frac{1}{M \times N} \sum_{i=0}^{M-1} \sum_{j=0}^{N-1} saturation_{ij} \\ con_l &= max(l) - min(l) \end{aligned}$$

here I have used  $c_1=0.4680$ ,  $c_2=0.2745$ ,  $c_3=0.2576$  as used in official implementation.

Ref-[Sow15]

### 5.3 Colorfulness,Contrast and Fog-density (CCF)

#### 5.3.1 Colorfulness Index

Underwater images suffer from serious color distortion because light attenuates a lot through water. Fu and Panetta demonstrate that we can use a combination of image statistics to represent colorfulness. During the process of calculating colorfulness index, as mentioned in [4], three

channels  $R(i,j)$ ,  $G(i,j)$ , and  $B(i,j)$  of a RGB underwater image are converted into logarithmic signals based on logarithmic-scale space. The conversion formulas are shown as follows,

$$R(i,j) = \log R(i,j) - \mu_R$$

$$G(i,j) = \log G(i,j) - \mu_G$$

$$B(i,j) = \log B(i,j) - \mu_B$$

where  $\mu_R, \mu_G, \mu_B$  are the mean values of  $\log R(i,j), \log G(i,j), \log B(i,j)$  respectively. Now define

$$\alpha = R - G$$

$$\beta = 0.5 \times (R + G) - B$$

$$\text{colorfulness} = \frac{\sqrt{\sigma_\alpha^2 + \sigma_\beta^2} + 0.3\sqrt{\mu_\alpha^2 + \mu_\beta^2}}{85.59}$$

where  $\sigma_\alpha^2, \sigma_\beta^2, \mu_\alpha, \mu_\beta$  are the variance and mean of  $\alpha$  and  $\beta$  channels.

### 5.3.2 Contrast Index

The degradation of underwater color images due to blurring caused by the scattering effect of water, particularly forward scattering. Blurring assessment is deemed crucial in evaluating the quality of these images. The approach presented involves dividing the underwater color image into 64x64 blocks and using edge detection with the Sobel operator to distinguish between edge and flat blocks. Edge blocks are identified based on whether the number of edge pixels exceeds 0.2% of the total pixels in a block. The blurring index of an underwater color image is then calculated as the sum of the RMS contrast values of all the identified edge blocks. The formula for calculating

the RMS contrast index is provided.

$$contrast = \sum_{i=1}^T \sqrt{\frac{1}{MN} \sum_{i=0}^{N-1} \sum_{j=0}^{M-1} (I_{ij} - \bar{I})^2}$$

where  $I_{ij}$  is the intensity of i,j th pixel in the image and  $\bar{I}$  is the average intensity of the pixel.

### 5.3.3 Fog Density Index

To predict the degree of a foggy scene from a natural image. This model calculates the deviations from statistical regularities obtained in fog-free images and foggy images. Finally, twelve features, which are extracted from nature scene statistical (NSS) model, such as offset brightness and entropy loss, are used to predict the fog density of an image. The mean vector  $\nu$  and the covariance matrix  $\Sigma$  are obtained by fitting all the statistical features extracted from the test image into multivariate Gaussian (MVG) model, which is calculated as follows,

$$MVG(f) = \frac{1}{(2\pi)^{\frac{d}{2}} |\Sigma|^{\frac{d}{2}}} \exp \left( -\frac{1}{2} (f - \nu)^t \Sigma^{-1} (f - \nu) \right)$$

where  $f$  is a d-dimensional feature vector representing statistical features and  $t$  indicates transposition. Then the foggy level  $D_f$  can be calculated by measuring the Mahalanobis distance between the MVG model of the test image and the MVG model of 500 natural fog-free images. Similarly, the fog-free level  $D_{ff}$  can be calculated by measuring the Mahalanobis distance between the MVG model of the test image and the MVG model of 500 foggy images. For example, the  $D_f$  can be calculated as follows,

$$D_f(v_1, v_2, \Sigma_1, \Sigma_2) = \sqrt{(v_1 - v_2)^t \left( \frac{\Sigma_1 + \Sigma_2}{2} \right)^{-1} (v_1 - v_2)}$$

where  $v_1, v_2$  and  $\Sigma_1, \Sigma_2$  represent the mean vector and the covariance matrices of the two MVG models, respectively. Finally, the fog density index of an image can be calculated as follows,

$$D = \frac{D_f}{1 + D_{ff}}$$

Now the CCF can be calculated as the weighted sum of these three quantities as follows

$$CCF = \omega_1 \times Colorfulness + \omega_2 \times Contrast + \omega_3 \times Fogdensity$$

here I have used  $\omega_1 = 0.17593, \omega_2 = 0.61759, \omega_3 = 0.33988$  as suggested by the original paper.

Ref-[Men18]

## 5.4 Entropy

For defining the entropy we represent the discrete information source as Markov process . Can we define a quantity which will measure, in some sense, how much information is “produced” by such a process, or better, at what rate information is produced? Suppose we have a set of possible events whose probabilities of occurrence are  $p_1, p_2, \dots, p_n$ . These probabilities are known but that is all we know concerning which event will occur. Can we find a measure of how much “choice” is involved in the selection of the event or of how uncertain we are of the outcome? If there is a such measure say  $H(p_1, p_2, \dots, p_n)$ . It is reasonable to require of it the following properties:-

1.  $H$  should be continuous in  $p_i$ .
2. if all the  $p_i$  are equal,  $p_i = \frac{1}{n}$  then  $H$  should be monotonic increasing function of  $n$ . With equally likely events there is more choices or uncertainty, when there are more possible ways.
3. If a choice be broken down into two successive choices, the original  $H$  should be the weighted sum of the individual values of  $H$ .

The only possible function satisfies all these axioms is

$$H = - \sum_{i=1}^n p_i \log p_i$$

for calculating the entropy of an image we first calculate the histogram of each channel of the image. Then we divide all the frequencies by the total number of total pixels in the image. Then we apply the above formula and sum up all the entropies.

Ref-[SHA48]

# Chapter 6

## Bayesian Retinex Underwater Image Enhancement

The proposed algorithm in the paper [Wu21] utilizes both Retinex theory and Bayes theory of probabilities to enhance the underwater images. It first applies a color correction on the image as described in chapter 3. After the color correction it converts the image from other formats to HSV format as described in chapter 2. we construct the model as given below.

### 6.1 Model Construction

#### 6.1.1 Step 1 : Color Correction :-

for each channel in RGB image do the color correction according to the given formula :-

$$U^c = \frac{255}{2} \left( 1 + \frac{S^c - M^c}{\mu V^c} \right)$$

where  $S^c$  = Color channel having values in [0,1].

$M^c$  = Mean of the channel .

$V^c$  = Variance of the channel.

### 6.1.2 Step 2 : RGB to HSV conversion :-

Digital color images has 3 color channels R,G,B . Every value of RGB channels lies between 0 to 255 including both 0 and 255. RGB stands for RED, GREEN, BLUE and HSV stands for HUE, SATURATION, VALUE

#### conversion from RGB to HSV :-

$$R' = R/255, G' = G/255, B' = B/255$$

$$cmax = \max(R', G', B'),$$

$$cmin = \min(R', G', B')$$

$$\Delta = cmax - cmin$$

$$H = \begin{cases} 60 \times \left( \frac{G' - B'}{\Delta} \mod 6 \right) & \text{if } cmax = R' \\ 60 \times \left( \frac{B' - R'}{\Delta} + 2 \right) & \text{if } cmax = G' \\ 60 \times \left( \frac{R' - G'}{\Delta} + 4 \right) & \text{if } cmax = B' \end{cases}$$

$$S = \begin{cases} 0 & \text{if } cmax = 0 \\ \frac{\Delta}{cmax} & \text{if } cmax \neq 0 \end{cases}$$

$$V = cmax$$

### 6.1.3 Step 3 : Model Description :-

Now select the V channel and let L=V ,  $L = L \times 255$  . By Retinex theory,  $L = I \circ R$  where  $R$  is Reflectance and  $I$  is Illumination.  $\circ$  is the element wise multiplication.

$$I_{ij} \in [0, 255]$$

$$R_{ij} \in [0, 1]$$

Now consider L,I,R as Random Variables then :-

$$p(L, I|R) \propto p(L|R, I)p(I)p(R)$$

where  $p(L|R, I)$  is the likelihood of  $L$  given  $R$  and  $I$ ,  $p(I)$  is the prior of  $I$  and  $p(R)$  is the prior of  $R$ . Now considers that  $p(L|R, I)$  follows the standard multivariate Normal distribution for given errors are zero. Priors for R and I are considered as product of two priors. Prior1 of R follows the laplacian distribution of first order gradient of R and Prior 2 follows the 2nd order gradient of the R. Similarly we assume that the Prior of I is the product of two Priors which are prior1 of first order gradient of I which follows standard multivariate Normal distribution and prior2 of the 2nd order gradient of I which follows standard multivariate Normal distribution :-

$$e = L - I \circ R$$

$$p(L|I, R) \sim \mathcal{N}(e|0, \sigma^2 I)$$

$$p_1(R) \sim \mathcal{L}(\nabla R|0, s_1 I)$$

$$p_2(R) \sim \mathcal{L}(\Delta R|0, s_2 I)$$

$$p(R) = p_1(R)p_2(R)$$

$$p_3(I) \sim \mathcal{N}(\nabla I|0, \sigma_1^2 I)$$

$$p_4(I) \sim \mathcal{N}(\Delta I|0, \sigma_2^2 I)$$

$$p(I) = p_3(I)p_4(I)$$

where  $\mathcal{N}$  is the Gaussian distribution and  $\mathcal{L}$  is the Laplacian distribution.

$$\nabla_h = [-1, 1], \nabla_v = \begin{bmatrix} -1 \\ 1 \end{bmatrix}$$

$$\Delta = \begin{bmatrix} 0 & -1 & 0 \\ -1 & 4 & -1 \\ 0 & -1 & 0 \end{bmatrix}$$

$$\mathcal{L}(x|\mu, b) = \frac{1}{2b} \exp\left(-\frac{|x - \mu|}{b}\right)$$

$$\mathcal{N}(x|\mu, \sigma^2) = \frac{1}{\sqrt{2\pi}\sigma} \exp\left(-\frac{(x - \mu)^2}{2\sigma^2}\right)$$

#### 6.1.4 Step 4 : Objective Function :-

Since we want to maximize the probability of  $p(L, I|R)$  so we will minimize the negative log likelihood of  $p(L, I|R)$ .

$$\mathcal{L}(L, I, R) = -\log p(L, I|R)$$

$$\mathcal{L}(L, I, R) = -\log p(L|R, I)p(I)p(R)$$

$$\mathcal{L}(L, I, R) = -\log p(L|R, I) - \log p(I) - \log p(R)$$

$$\mathcal{L}(L, I, R) = -\log p(L|R, I) - \log p(I) - \log p_1(R) - \log p_2(R)$$

$$\mathcal{L}(L, I, R) = -\log p(L|R, I) - \log p_3(I) - \log p_4(I) - \log p_1(R) - \log p_2(R)$$

$$\begin{aligned} \mathcal{L}(L, I, R) &= -\sum \sum \log \frac{1}{\sqrt{2\pi}\sigma} \exp\left(-\frac{(I_{ij} \circ R_{ij} - L_{ij})^2}{2\sigma^2}\right) - \sum \sum \log \frac{1}{\sqrt{2\pi}\sigma_1} \exp\left(-\frac{(\nabla I_{ij})^2}{2\sigma_1^2}\right) \\ &\quad - \sum \sum \log \frac{1}{\sqrt{2\pi}\sigma_2} \exp\left(-\frac{(\Delta I_{ij})^2}{2\sigma_2^2}\right) - \sum \sum \log \frac{1}{2s_1} \exp\left(-\frac{|\nabla R_{ij}|}{s_1}\right) - \sum \sum \log \frac{1}{2s_2} \exp\left(-\frac{|\Delta R_{ij}|}{s_2}\right) \\ \mathcal{L}(L, I, R) &= \sum \sum \frac{(I_{ij} \circ R_{ij} - L_{ij})^2}{2\sigma^2} + \sum \sum \frac{(\nabla I_{ij})^2}{2\sigma_1^2} + \sum \sum \frac{(\Delta I_{ij})^2}{2\sigma_2^2} + \sum \sum \frac{|\nabla R_{ij}|}{s_1} + \sum \sum \frac{|\Delta R_{ij}|}{s_2} \end{aligned}$$

+C

$$\mathcal{L}(L, I, R) = \|I \circ R - L\|_2^2 + \frac{\sigma^2}{2\sigma^2} \|\nabla I\|_2^2 + \frac{\sigma^2}{2\sigma_1^2} \|\Delta I\|_2^2 + \frac{\sigma^2}{s_1} \|\nabla R\|_1 + \frac{\sigma^2}{s_2} \|\Delta R\|_1 + C$$

$$\mathcal{E}(I, R) = \|I \circ R - L\|_2^2 + \frac{\sigma^2}{2\sigma^2} \|\nabla I\|_2^2 + \frac{\sigma^2}{2\sigma_1^2} \|\Delta I\|_2^2 + \frac{\sigma^2}{s_1} \|\nabla R\|_1 + \frac{\sigma^2}{s_2} \|\Delta R\|_1$$

$$\mathcal{E}(I, R) = \|I \circ R - L\|_2^2 + \nu_1 \|\nabla I\|_2^2 + \nu_2 \|\Delta I\|_2^2 + \nu_3 \|\nabla R\|_1 + \nu_4 \|\Delta R\|_1$$

where  $\nu_1 = \frac{\sigma^2}{2\sigma^2}$ ,  $\nu_2 = \frac{\sigma^2}{2\sigma_1^2}$ ,  $\nu_3 = \frac{\sigma^2}{s_1}$ ,  $\nu_4 = \frac{\sigma^2}{s_2}$  and  $C$  is a constant.

### 6.1.5 Step 5 : Numerical Optimization :-

To optimize the objective function . We have to convert  $l_1$  norm to  $l_2$  norm. We introduce two auxiliary variables  $d, h$  and two error terms  $m, n$ .

$$\begin{aligned}\mathcal{E}(I, R) &= \|I \circ R - L\|_2^2 + \nu_3 \|\nabla I\|_2^2 + \nu_4 \|\Delta I\|_2^2 + \nu_1 \|\nabla R\|_1 + \nu_1 \|\Delta R\|_1 \\ \mathcal{E}(I, R) &= \|I \circ R - L\|_2^2 + \nu_3 \|\nabla I\|_2^2 + \nu_4 \|\Delta I\|_2^2 \\ &\quad + \nu_1 (\|d\|_1 + \lambda_1 \|\nabla R - d + m\|_2^2) + \nu_1 (\|h\|_1 + \lambda_2 \|\Delta R - h + n\|_2^2)\end{aligned}$$

Now we split this into three parts and optimize it using ADMM algorithm →

P-1

$$\begin{aligned}d^k &= \arg \min_d (\|d\|_1 + \lambda_1 \|\nabla R^{k-1} - d + m^{k-1}\|_2^2) \\ h^k &= \arg \min_h (\|h\|_1 + \lambda_2 \|\Delta R^{k-1} - h + n^{k-1}\|_2^2)\end{aligned}$$

P-2

$$\begin{aligned}R^k &= \arg \min_R \left( \|R - \frac{L}{I^{k-1}}\|_2^2 + \nu_1 \lambda_1 \|\nabla R - d^k + m^{k-1}\|_2^2 + \nu_2 \lambda_2 \|\Delta R - h^k + n^{k-1}\|_2^2 \right) \\ m^k &= m^{k-1} + \nabla R^k - d^k \\ n^k &= n^{k-1} + \Delta R^k - h^k\end{aligned}$$

P-3

$$I^k = \arg \min_I \left( \|I - \frac{L}{R^k}\|_2^2 + \nu_3 \|\nabla I\|_2^2 + \nu_4 \|\Delta I\|_2^2 \right)$$

### 6.1.6 Step 6 : Update for P-1 :-

$$d_h^k = \text{shrink}(\nabla_h R^{k-1} + m_h^{k-1}, \frac{1}{2\lambda_1})$$

$$d_v^k = \text{shrink}(\nabla_v R^{k-1} + m_v^{k-1}, \frac{1}{2\lambda_1})$$

$$h^k = \text{shrink}(\Delta R^{k-1} + n^{k-1}, \frac{1}{2\lambda_2})$$

where  $\text{shrink}(x, \gamma) = \max(0, |x| - \gamma) \times \frac{x}{|x|}$  and  $\frac{x}{|x|} = 0$  if  $x = 0$

### 6.1.7 Step 7 : Update for P-2 :-

$$R^k = \mathcal{F}^{-1} \left( \frac{\mathcal{F}(L/I^{k-1}) + \nu_1 \lambda_1 \Phi_1 + \nu_2 \lambda_2 \Phi_2}{1 + \nu_1 \Psi_1 + \nu_2 \Psi_2} \right)$$

where  $\Phi_1 = \mathcal{F}^*(\nabla_h) \cdot \mathcal{F}(d_h^k + m_h^{k-1}) + \mathcal{F}^*(\nabla_v) \cdot \mathcal{F}(d_v^k + m_v^{k-1})$  and

$$\Phi_2 = \mathcal{F}^*(\Delta) \cdot \mathcal{F}(h^k + n^{k-1})$$

$\Psi_1 = \mathcal{F}^*(\nabla_h) \cdot \mathcal{F}(\nabla_h) + \mathcal{F}^*(\nabla_v) \cdot \mathcal{F}(\nabla_v)$  and

$\Psi_2 = \mathcal{F}^*(\Delta) \cdot \mathcal{F}(\Delta)$   $\mathcal{F}$  is FFT Operator

$$m_h^k = m_h^{k-1} + \nabla R_h^k - d_h^k$$

$$m_v^k = m_v^{k-1} + \nabla R_v^k - d_v^k$$

$$n^k = n^{k-1} + \Delta R^k - h^k$$

### 6.1.8 Step 9 : Update for P-3 :-

$$I^k = \mathcal{F}^{-1} \left( \frac{\mathcal{F}(\frac{L}{R^k})}{\mathcal{F}(1) + \nu_3 \Psi_3 + \nu_4 \Psi_4} \right)$$

### 6.1.9 Algorithm :-

**Input** : – input value channel L, weighting parameters  $\nu_1, \nu_2, \nu_3, \nu_4$  and  $\lambda_1, \lambda_2$  and the number of iterations T

**Initialization** : – initialize  $\mathbf{I}^0 = \text{Gaussian filter of } L$   $\mathbf{R}^0 = \mathbf{0}$  and

$d_h^0 = d_v^0 = h_h^0 = h_v^0 = m_h^0 = m_v^0 = n_h^0 = n_v^0 = 0$  and k=1

**Iteration on k** : – repeat until k=T :

update  $d_h^k, d_v^k, h_h^k, h_v^k$  using update for P-1;

update  $R^k$  using update for P-2

update  $m_h^k, m_v^k, n^k$  using update for P-2;

update  $I^k$  using update for P-3

**Stopping Criteria** : – terminate iteration if k=T otherwise continue iteration k=k+1;

**Output** : – output the reflectance R and illumination I

### 6.1.10 Gamma Correction :-

$$I_e = W \times \left( \frac{I}{W} \right)^{\frac{1}{\gamma}}$$

use W = 250 and  $\gamma = 2.5$

### 6.1.11 Image Reconstruction :-

$$L_e = I_e \circ R_e$$

now convert the image from HSV to RGB by using the formula given below .

### 6.1.12 Conversion from HSV to RGB :-

$$C = V \times S$$

$$X = C \times \left( 1 - \left| \left( \frac{H}{60} \bmod 2 \right) - 1 \right| \right)$$

$$m = V - C$$

$$\begin{cases} (R', G', B') = (C, X, 0) & \text{if } 0 \leq H < 60 \\ (R', G', B') = (X, C, 0) & \text{if } 60 \leq H < 120 \\ (R', G', B') = (0, C, X) & \text{if } 120 \leq H < 180 \\ (R', G', B') = (0, X, C) & \text{if } 180 \leq H < 240 \\ (R', G', B') = (X, 0, C) & \text{if } 240 \leq H < 300 \\ (R', G', B') = (C, 0, X) & \text{if } 300 \leq H < 360 \end{cases}$$

$$(R, G, B) = (R' + m, G' + m, B' + m)$$

In the implementation I have used  $\nu_1 = 1, \nu_2 = 10^{-3}, \nu_3 = 10^{-5}, \nu_4 = 10^{-3}, \lambda_1 = 10^{-4}, \lambda_2 = 10^{-3}, K = 4, \mu = 2.5$ (adjustable) as suggested by the author.

Ref-[Wu21]

## 6.2 Results

### 6.2.1 Comparison with other algorithms

In the figure 6.1 and 6.2 we can see the enhanced and raw image. In the figure 6.3 I have shown the raw and processed image further from the figure 6.4 to figure 6.4 we can see the same image as figure 6.3 enhanced by different images. The implementation of the algorithms can be found in the github repo(link given in the conclusion). In the table 6.1 the comparison of the different

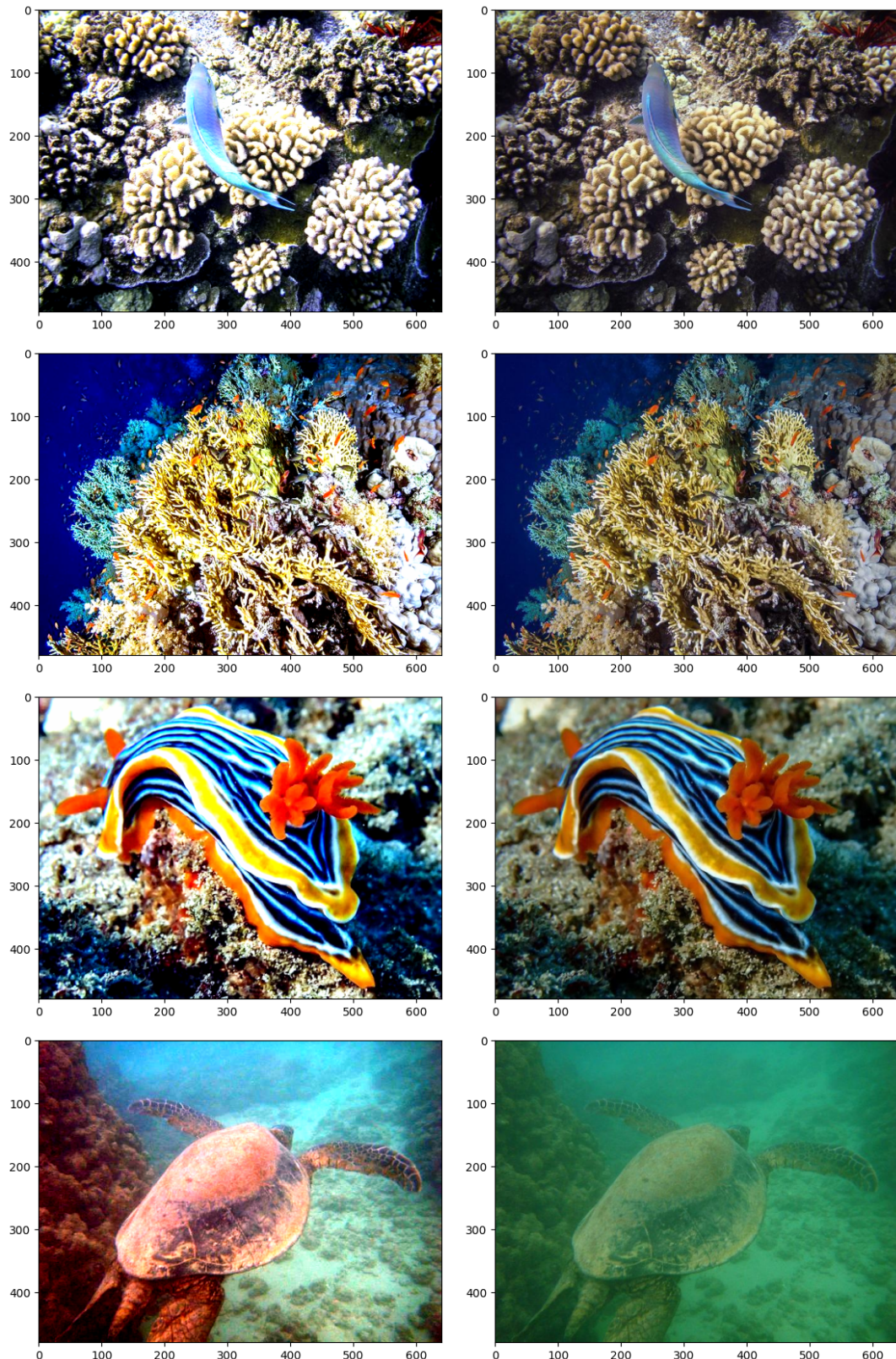


**Fig. 6.1:** right unprocessed and left processed

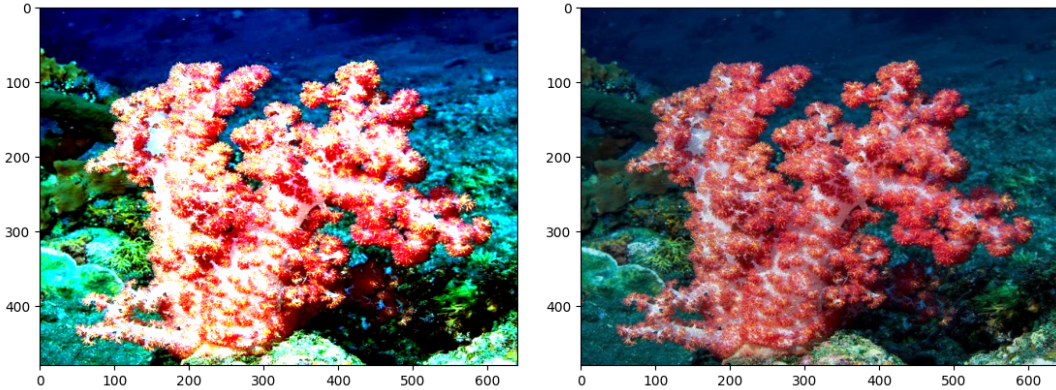


**Fig. 6.2:** right unprocessed and left processed

metrics are given for the different algorithms . All the metrics are the average values of the 31 different images. In the figure 6.8 and figure 6.9 four enhanced images are given. In table 6.2 comparison of number of edges recovered by the different algorithms are given . Number of edges are calculated using Canny Edge detection [Can86] with threshold1=100 and threshold2=200 using OpenCV. In the original paper author have used different method for this purpose. From figure 6.10 to figure 6.13 bar chart comparison is given for single image for each metric namely CCF, UCIQE,UICM,UIConM,UIQM and UISM.

### 6.2.2 List algorithms for comparison

- Contrast Limited adaptive Histogram Equalization (CLAHE) .
- Grey World .
- Max RGB.
- Multiscale Retinex and Single Scale Retinex (MSR and SSR) .
- Multiscale Retinex with Color Restoration (MSRCR).
- Multiscale Retinex with chromaticity preservation (MSRCP) .
- Wavelength Compensation Image Dehazing (WCID).

- White Balance.

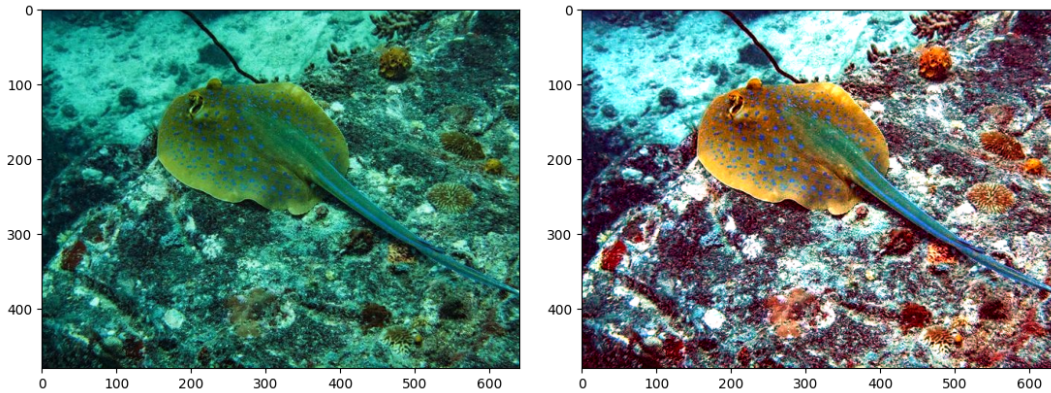


**Fig. 6.3:** raw and processed image

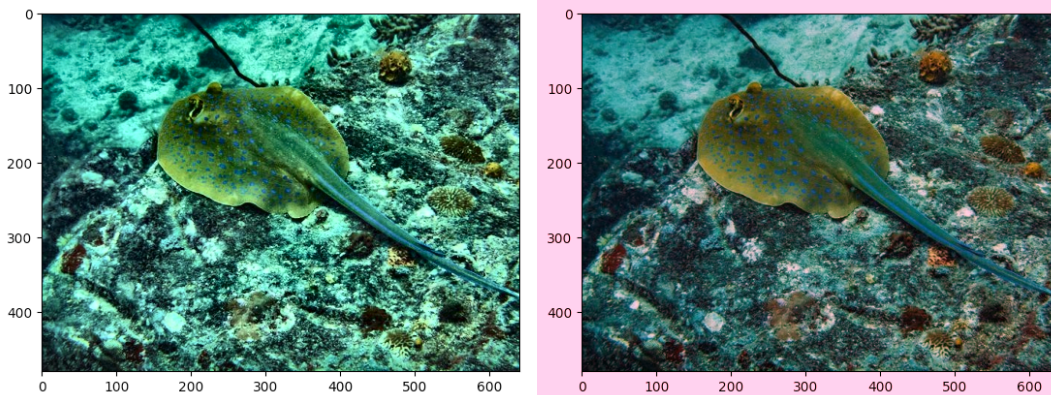


**Fig. 6.4:** Clahe [vas13] and Grey World [Buc80]

**Table 6.1:** Comparison of Image Processing Methods

Method	UCIQE	UIQM	UIConM	UISM	UICM	Entropy	CCF
Raw	34.5435	0.9638	-0.1489	4.0165	10.9910	6.4360	6.1078
Processed	36.1423	1.3170	-0.1368	4.8742	13.0017	6.7837	12.9806
Clahe	34.2644	1.2024	-0.1560	4.9006	11.1018	6.7788	11.365
Grey World	30.8121	0.9518	-0.1493	3.9647	11.1663	6.4246	6.5771
Max RGB	27.3190	0.9303	-0.1473	4.3682	5.9217	6.5853	2.852
MSR	34.5479	1.3611	-0.1393	5.1399	12.1020	7.7569	17.6559
MSRCP	38.2102	1.0643	-0.1327	4.4564	7.8934	7.0115	5.1098

MSRCR	15.0838	0.7142	-0.1198	3.8844	-0.1653	6.0080	2.3201
SSR	36.0846	1.2733	-0.1338	4.8325	11.5080	7.0979	19.3236
WCID	32.6000	0.7255	-0.0979	2.5337	11.6125	4.3645	12.4484
White Balance	34.9375	0.8975	-0.1495	3.8324	10.6460	6.3755	7.1807

**Table 6.2:** Recovered Edges by different algorithms

	Image A	Image B	Image C	Image D
Clahe	38020	51369	18999	17576
Grey World	19387	36991	10709	8438
Max RGB	21602	38101	10566	8929
MSR	36897	55918	22716	18669
MSRCP	13458	41676	10444	6818
MSRCR	5300	4512	4402	4159
Processed	38291	43419	17687	15331
Raw	21127	37759	9440	8196
SSR	37285	48639	16494	14904
WCID	10238	23330	7293	5832
White Balance	20123	37840	11066	9094

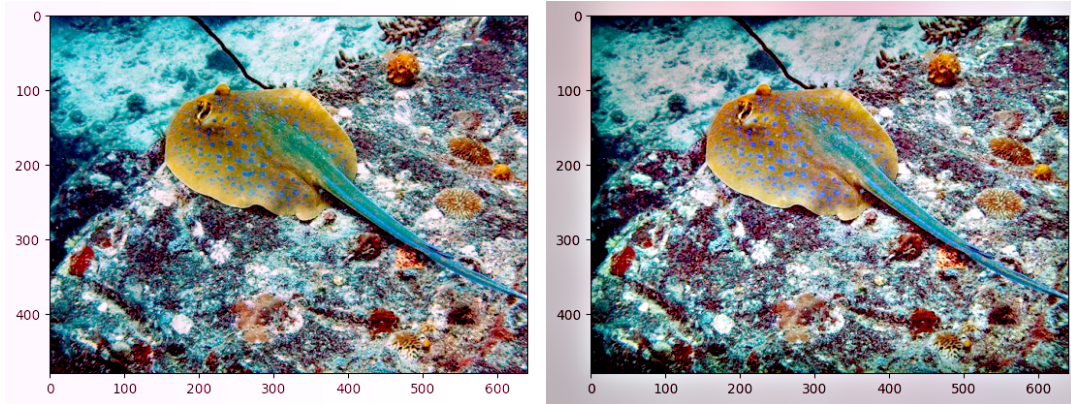


**Fig. 6.5:** SSR [Job15a] and MSR [Job15b]

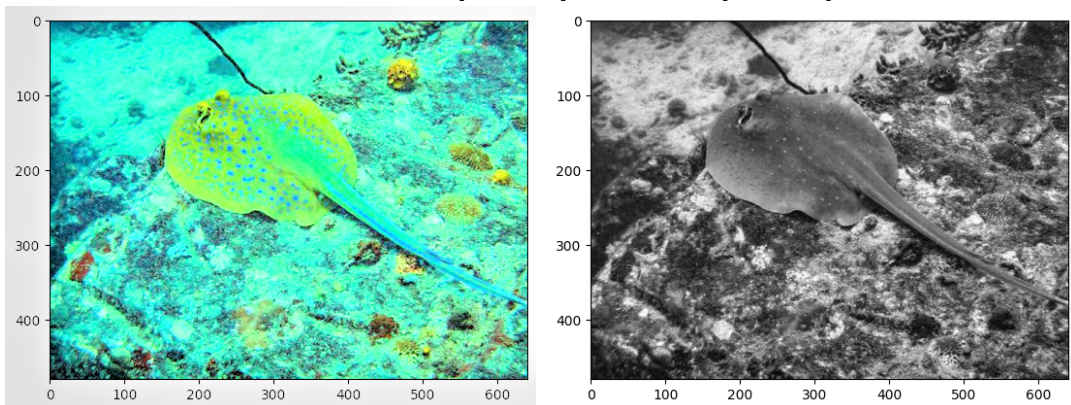


**Fig. 6.6:** MSRCP [San12] and MAXRGB [Lan77]

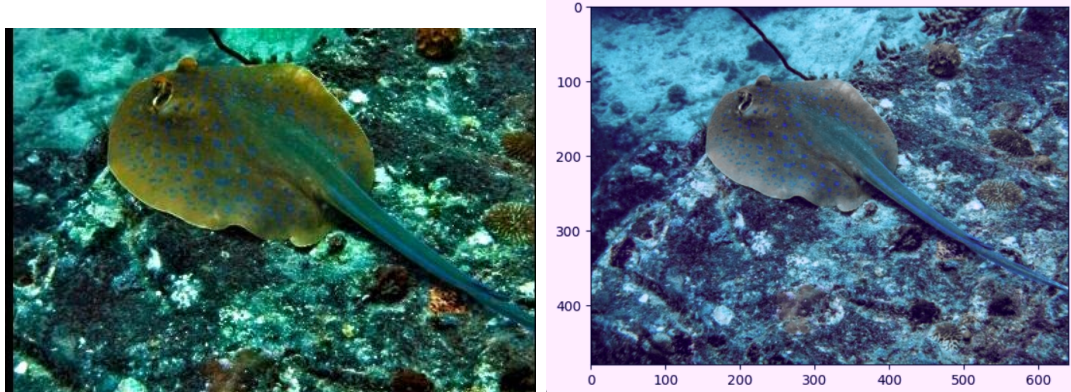


**Fig. 6.7:** WCID [CC12] and white balance [M07]

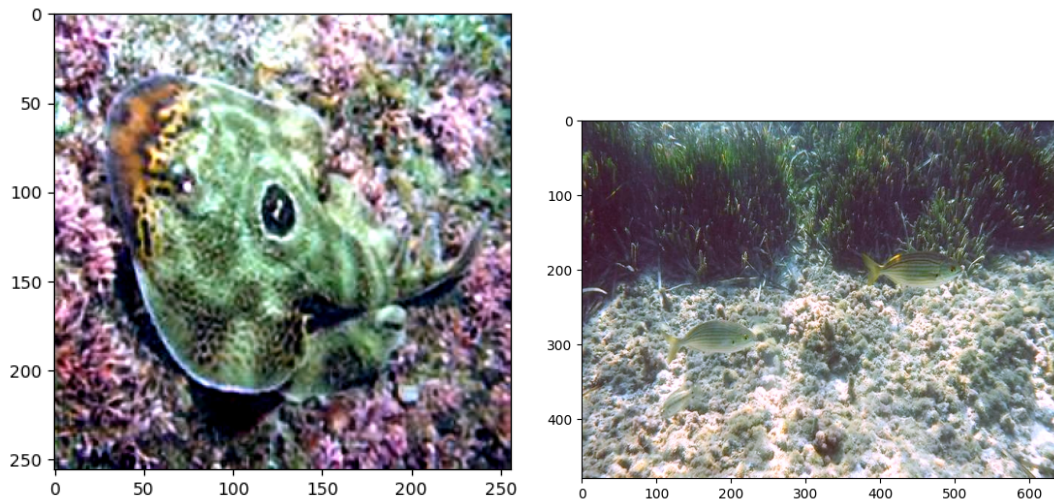


**Fig. 6.8: (A) & (B)**

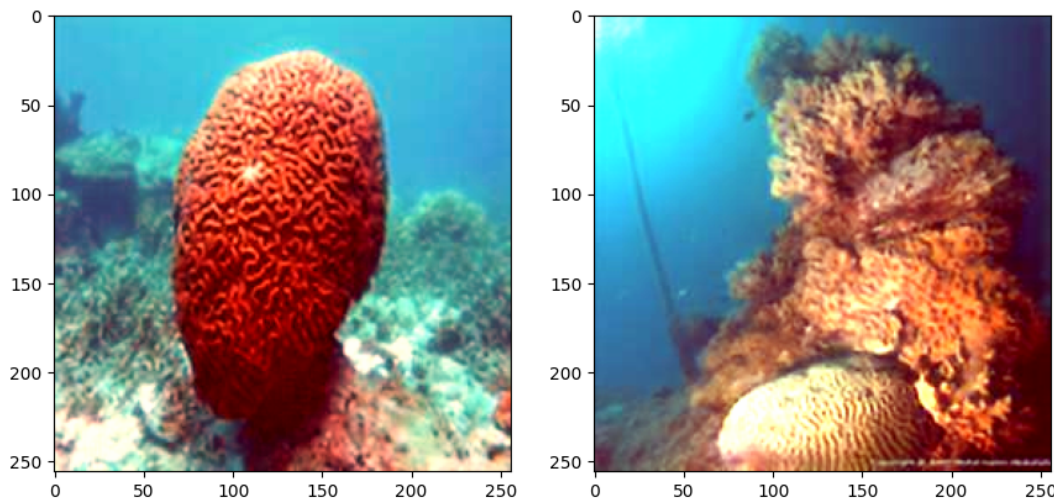


**Fig. 6.9: (C) & (D)**

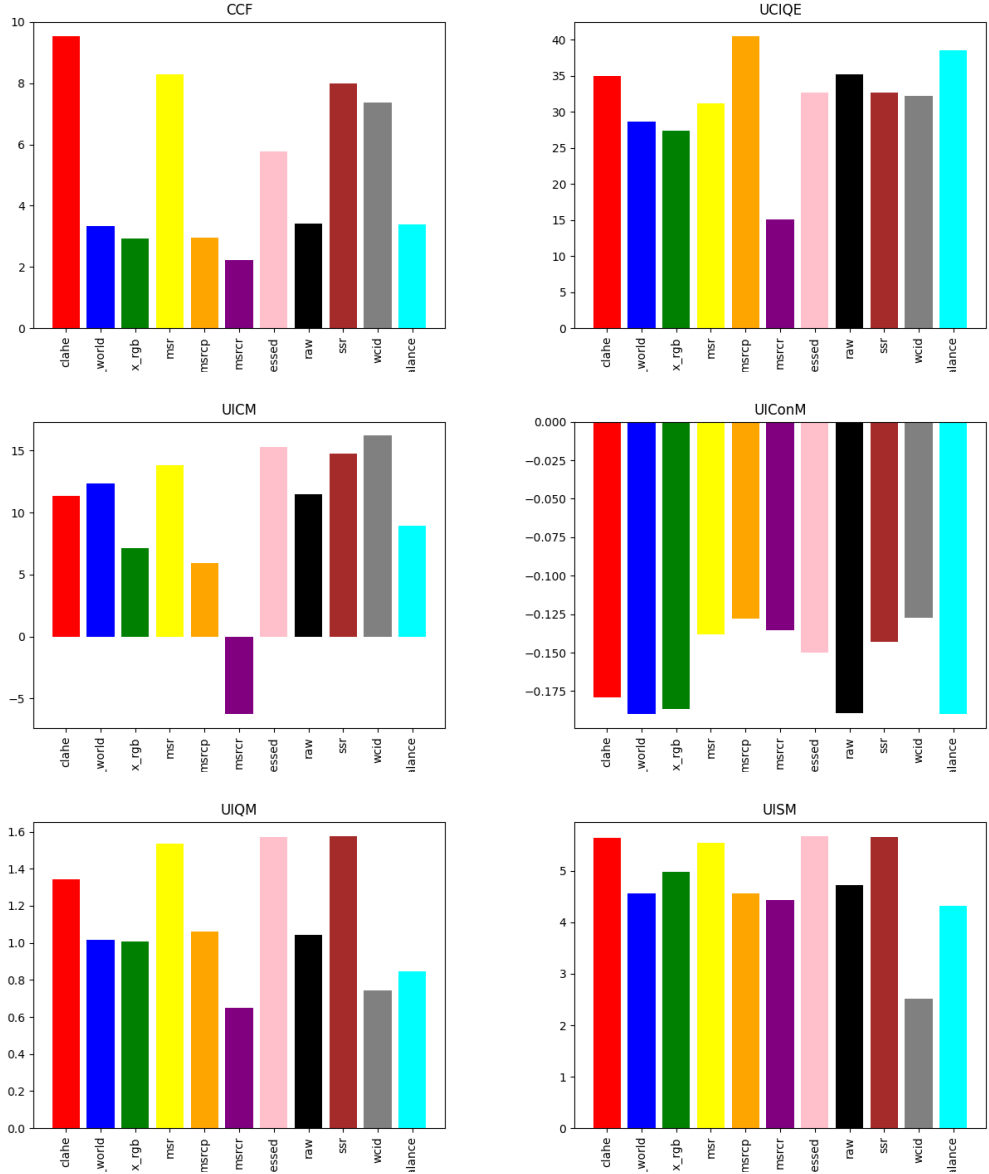


**Fig. 6.10:** for image A

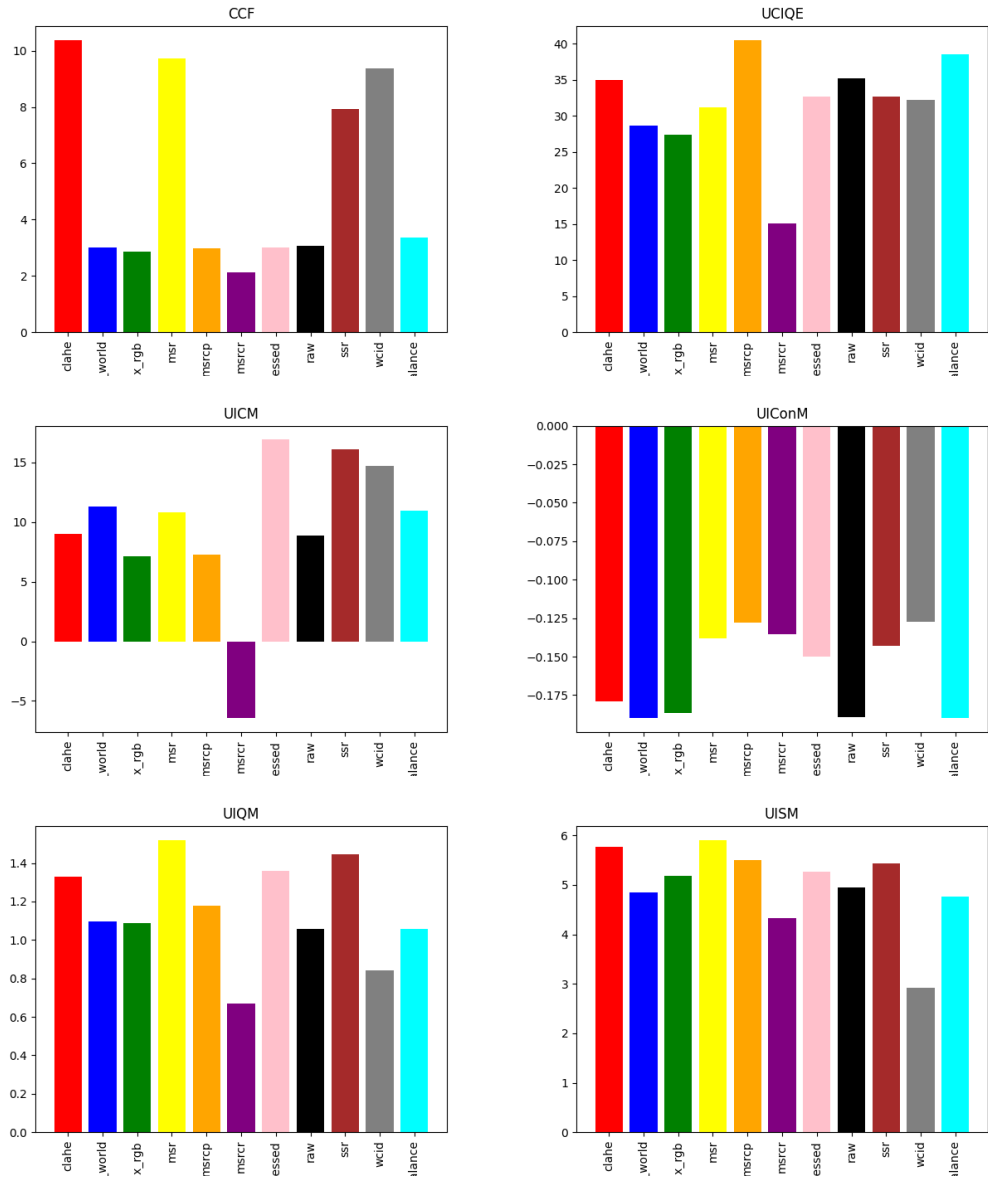


**Fig. 6.11:** for image B

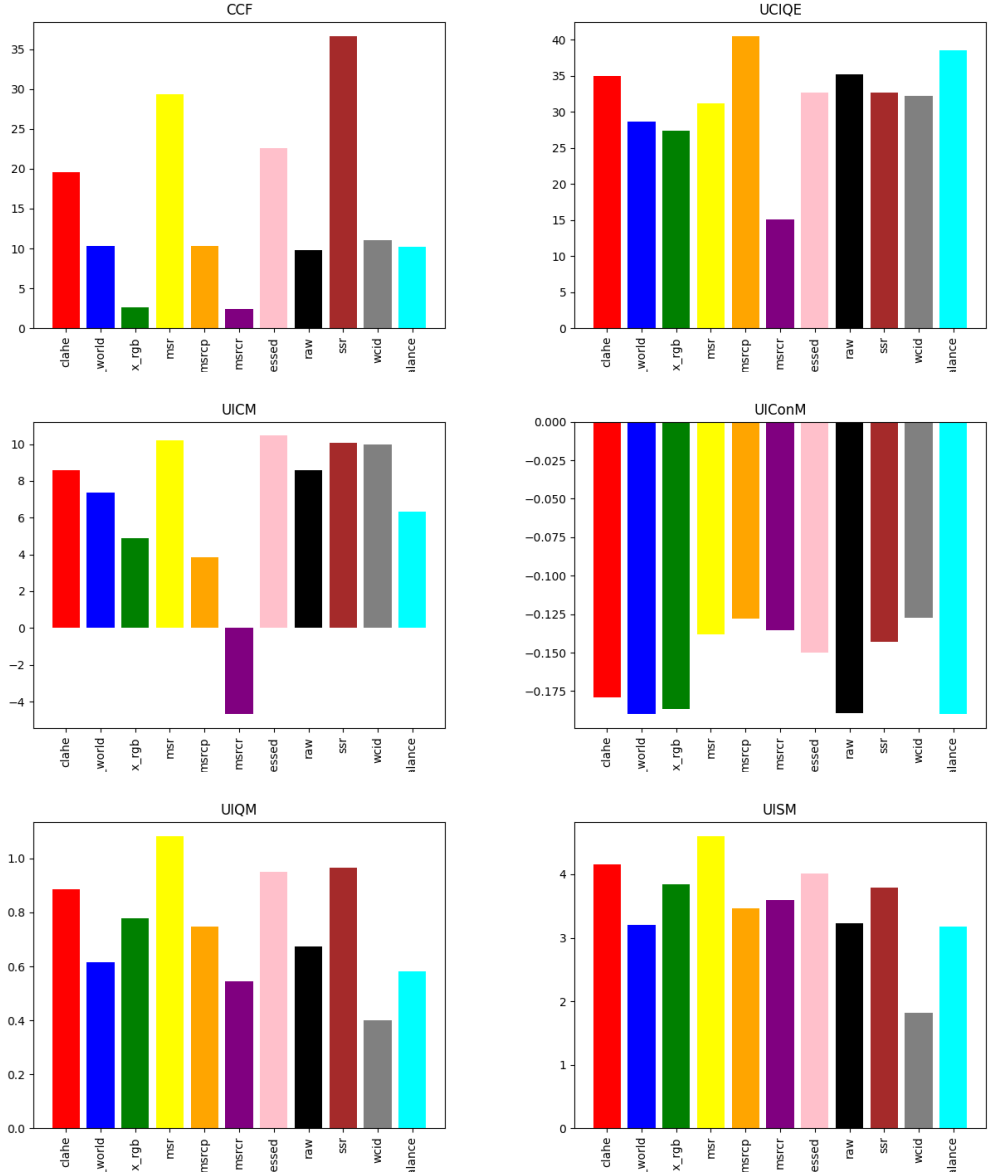


**Fig. 6.12:** for image C

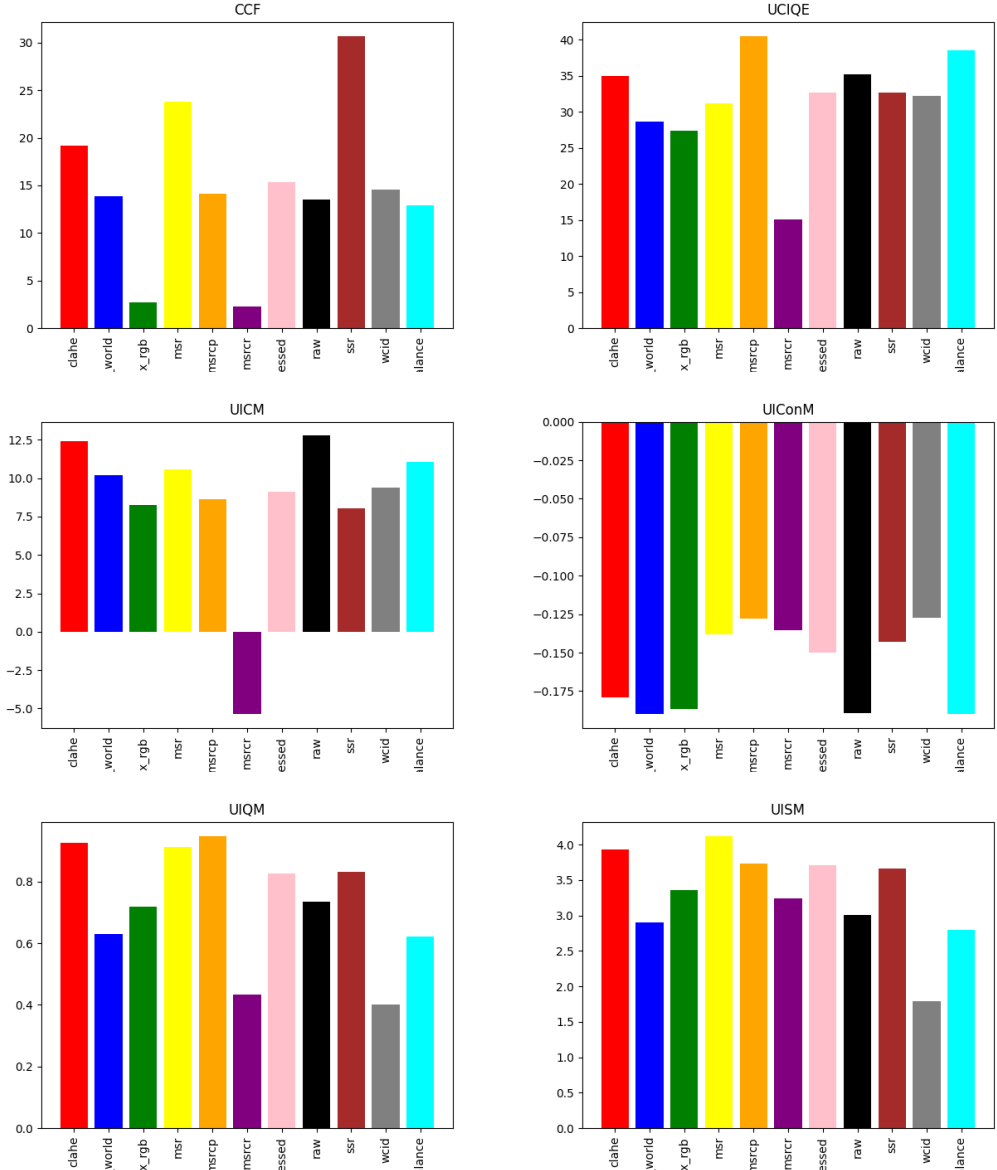


**Fig. 6.13:** for image D

# Chapter 7

## Conclusion and Future Work

### 7.1 Conclusion

It uses a simple but effective color correction approach to remove color casts and restore natural colors, which can serve as a preprocessing step for other underwater enhancement methods. It establishes a Bayesian retinex enhancement model with multiorder gradient priors (first and second order) on both the reflectance and illumination components. This captures fine details and structures better by modeling spatial smoothness and linear approximations. The complex problem is decomposed into three simpler denoising subproblems that are solved via an efficient alternating optimization algorithm, providing mathematical convergence analysis. The model performs pixel-wise operations without requiring prior knowledge of underwater imaging conditions. Comprehensive analyses demonstrate the method’s effective performance in terms of color accuracy, handling challenging scenes, parameter evaluations, algorithm convergence, and improvement over baseline methods based on an ablation study. Overall, the proposed Bayesian retinex model with multiorder gradient priors shows robust and promising performance for single underwater image enhancement.

## 7.2 Future Work

For future work, I am planning to explore deep learning based approaches for underwater image enhancement, specifically methods like MDGAN (Multi-Decoder Generative Adversarial Network) and UGAN (Underwater Generative Adversarial Network). These techniques leverage the power of generative adversarial networks (GANs) and convolutional neural networks (CNNs) to learn a non-linear mapping between degraded underwater images and their enhanced counterparts from large training datasets.

MDGAN employs multiple decoupled decoders to separately recover the three color channels, allowing the network to better capture the unique distortions in each channel. UGAN introduces a underwater image degradation model as a domain translation process, learning a mapping between rendered underwater style images and their corresponding clear versions.

\* all the images and code can be found in the given github repo. <https://github.com/rahim-khan-iitg/underwater-image-enhancement.git>



# References

- [Aga16] Karen Panetta; Chen Gao; Sos Agaian. Human-visual-system-inspired underwater image quality measures. *IEEE Journal of Oceanic Engineering*, July 2016.
- [Buc80] G. Buchsbaum. A spatial processor model for object colour perception. *Journal of the Franklin Institute*, July 1980.
- [Bur09] Wilhelm Burger ; Mark J. Burge. Principles of digital image processing fundamental techniques. *Springer-Verlag*, 2009.
- [Can86] John Canny. A computational approach to edge detection. *IEEE Transactions on Pattern Analysis and Machine Intelligence*, Nov 1986.
- [CC12] John Y. Chiang and Ying-Ching Chen. Underwater image enhancement by wavelength compensation and dehazing. *IEEE TRANSACTIONS ON IMAGE PROCESSING*, 2012.
- [Din14] Xueyang Fu; Peixian Zhuang; Yue Huang; Yinghao Liao; Xiao-Ping Zhang; Xinghao Ding. A retinex-based enhancing approach for single underwater image. *IEEE International Conference on Image Processing (ICIP)*, oct 2014.
- [Job15a] Bo Jiang; Glenn A. Woodell; Daniel J. Jobson. Novel multi-scale retinex with color restoration on graphics processing unit. *Springer Link*, 2015.
- [Job15b] Bo Jiang; Glenn A. Woodell; Daniel J. Jobson. Novel multi-scale retinex with color restoration on graphics processing unit. *Springer Link*, 2015.

- [Lan77] E.H Land. Maximum response in each channel of rgb caused by a white patch. *Sci. Amer.*, 1977.
- [M07] Ebner M. Color constancy. *wiley*, 2007.
- [Men18] Wang Yan; Li Na ; Li Zongying ; Gu Zhaorui; Zheng Haiyong; Zheng Bing ; Sun Mengnan. An imaging-inspired no-reference underwater color image quality assessment metric. *Computers Electrical Engineering*, Aug 2018.
- [PE10] S. Boyd; N. Parikh; E. Chu; B. Peleato; and J. Eckstein. Distributed optimization and statistical learning via the alternating direction method of multipliers. *Foundations and Trends in Machine Learning*, Nov 2010.
- [San12] Sudharsan Parthasarathy; Praveen Sankaran. An automated multi scale retinex with color restoration for image enhancement. *2012 National Conference on Communications (NCC)*, 2012.
- [SHA48] C. E. SHANNON. A mathematical theory of communication. *The Bell System Technical Journal*, 1948.
- [Sow15] Miao Yang; Arcot Sowmya. An underwater color image quality evaluation metric. *IEEE Transactions on Image Processing*, Oct 2015.
- [vas13] vasamsetti. Contrast limited adaptive histogram equalization. *Science Direct*, 2013.
- [Wu21] Peixian Zhuang; Chongyi Li ; Jiamin Wu. Bayesian retinex underwater image enhancement. *Engineering Applications of Artificial Intelligence*, Jan 2021.